of a metalated bismuth alkyl complex.

Acknowledgment. We thank the National Science Foundation (Grant CHE 8806205), the Robert A. Welch Foundation, and the Alexander von Humboldt Stiftung for support of this work. We also gratefully acknowledge the NSF for support in the purchase of the Rigaku AFC5S automated diffractometer.

Supplementary Material Available: Tables of complete crystallographic data collection parameters, positional parameters and isotropic thermal parameters for the $[Et_4N]^+$ cations in IIa and IIb, anisotropic thermal parameters for IIa, IIb, and III, and additional bond parameters for IIa and IIb (16 pages); tables of observed and calculated structure factors for IIa, IIb, and III (86 pages). Ordering information is given on any current masthead page.

Contribution from the Laboratoire de Chimie Inorganique, URA No. 420, and Institut d'Electronique Fondamentale, URA No. 022, Université de Paris-Sud, 91405 Orsay, France, and Department of Chemistry, University of Bergen, 5007 Bergen, Norway

Magnetism of Alternating Bimetallic Chains: Application to $MnCu(obzp)(H_2O)_3 \cdot H_2O$ (obzp = Oxamido-*N*-benzoato-*N'*-propionato)

Yu Pei,[1a] Keitaro Nakatani,[1a] Olivier Kahn,*[,1a] Jorunn Sletten,[1b] and Jean Pierre Renard[1c]

Received December 21, 1988

Two new alternating bimetallic chain compounds have been synthesized. Their formulas are $MnCu(obzp)(H_2O)_3 \cdot H_2O$ (**1**), with obzp = oxamido-*N*-benzoato-*N'*-propionato, and $MnCu(ophp) \cdot 5H_2O$ (**2**), with ophp = oxamido-*N*-phenolato-*N'*-propionato. **1** and **2** have been obtained by reaction of the Mn(II) ion with the dissymmetrical copper(II) brick $[Cu(obzp)]^{2-}$ or $[Cu(ophp)]^{2-}$. The crystal structure of **1** has been determined. It crystallizes in the monoclinic system, space group $P2_1/n$, with $a = 7.814$ (1) Å, $b = 10.3375$ (7) Å, $c = 19.981$ (1) Å, $\beta = 98.43$ (1)°, and $Z = 4$ (MnCu units). The structure consists of $Mn^{II}Cu^{II}$ chains with octahedral Mn(II) and square-planar Cu(II) bridged by oxamido (Mn···Cu = 5.4376 (6) Å) and carboxylato (Mn···Cu = 5.3670 (4) Å) groups. The configuration around the carboxylato bridge is of the anti–syn type, whereas it is of the anti–anti type in the previously reported alternating bimetallic chain compound $MnCu(obp)(H_2O)_3 \cdot H_2O$, with obp = oxamido-*N*,*N'*-bis-propionato). The $\chi_M T$ versus T plot, χ_M being the molar magnetic susceptibility per MnCu unit and T the temperature, has been measured in the 300–2 K temperature range. In spite of the chain structure, **1** does not behave as a ferrimagnetic chain but as an isolated $Mn^{II}Cu^{II}$ pair with an oxamido bridge. The quintet–septet energy gap was found equal to $3J = -82.2\ cm^{-1}$. The interaction parameter through the carboxylato bridge is negligible. This unexpected result is attributed to the anti–syn configuration around this bridge; the $d_{x^2-y^2}$ and d_{z^2} type magnetic orbitals on Mn(II), and the $d_{x^2-y^2}$ type magnetic orbital on Cu(II), are unfavorably oriented to interact. The magnetic behavior of **2** is very similar to that of **1**.

Introduction

For a couple of years, a new type of molecular-based materials has emerged, namely the molecular-based ferromagnets.[2,3] The first compounds of this kind have been reported. To our knowledge, three research teams have synthesized and fully characterized molecular-based compounds exhibiting a spontaneous magnetization below a critical temperature T_c.[4-10] Our specific strategy along this line consists of assembling ferrimagnetic chains within the crystal lattice in a ferromagnetic fashion.[6,9] This strategy led us to describe a new family of regular bimetallic chains, in which the nearest-neighbor metal centers are equally spaced[11] and then the first alternating bimetallic chains.[12,13] Alternating in the context means that there is alternation not only of the magnetic centers but also of the exchange pathways. Our synthetic approach to obtain $Mn^{II}Cu^{II}$ alternating bimetallic chains is schematized as

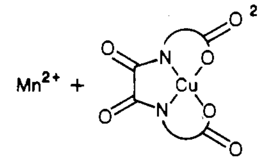

The Mn(II) ion reacts with a dianionic copper(II) precursor containing both oxamido and carboxylato groups capable of bridging the metal centers. So far, we have synthesized and utilized two copper(II) precursors of this kind, namely $[Cu(obp)]^{2-}$ and $[Cu(obbz)]^{2-}$ with obp = oxamido-*N*,*N'*-bis(propionato) and obbz = oxamido-*N*,*N'*-bis(benzoato). These two copper(II) dianions are symmetrical in the sense that, in addition to the molecular plane, there is a mirror plane perpendicular to the molecular plane. Their symmetry is expected to be close to C_{2v}. The former compound when reacting with Mn(II) gives $MnCu(obp)(H_2O)_3 \cdot H_2O$, which magnetically behaves as a ferrimagnetic

---

(1) (a) Laboratoire de Chimie Inorganique, Université de Paris-Sud. (b) University of Bergen. (c) Institut d'Electronique Fondamentale, Université de Paris-Sud.

(2) Miller, J. S.; Epstein, A. J.; Reiff, W. M. *Chem. Rev.* **1988**, *88*, 201; *Acc. Chem. Res.* **1988**, *21*, 114; *Science* **1988**, *240*, 40.

(3) Kahn, O. *Struct. Bonding (Berlin)* **1987**, *68*, 89; In *Organic and Inorganic Low-Dimensional Crystalline Materials*; Delhaes, P.; Drillon, M., Eds.; NATO ASI Series 168; Plenum: New York, 1987; p 93.

(4) Miller, J. S.; Epstein, A. J. *J. Am. Chem. Soc.* **1987**, *109*, 3850.

(5) Miller, J. S.; Calabrese, J. C.; Rommelmann, H.; Chittipeddi, S. R.; Zhang, J. H.; Reiff, W. M.; Epstein, A. J. *J. Am. Chem. Soc.* **1987**, *109*, 769.

(6) Kahn, O.; Pei, Y.; Verdaguer, M.; Renard, J. P.; Sletten, J. *J. Am. Chem. Soc.* **1988**, *110*, 782.

(7) Caneschi, A.; Gatteschi, D.; Renard, J. P.; Rey, P.; Sessoli, R. *Inorg. Chem.* **1989**, *28*, 1976.

(8) Lloret, F.; Nakatani, K.; Journaux, Y.; Kahn, O.; Pei, Y.; Renard, J. P.; *J. Chem. Soc., Chem. Commun.* **1988**, 642.

(9) Journaux, Y.; Van Koningsbruggen, P.; Lloret, F.; Nakatani, K.; Pei, Y.; Kahn, O.; Renard, J. P. *J. Phys., Colloq.* **1988**, *49* (C8), 851.

(10) Nakatani, K.; Carriat, J. Y.; Journaux, Y.; Kahn, O.; Lloret, F.; Renard, J. P.; Pei, Y.; Sletten, J.; Verdaguer, M. *J. Am. Chem. Soc.*, in press.

(11) Pei, Y.; Verdaguer, M.; Kahn, O.; Sletten, J.; Renard, J. P. *Inorg. Chem.* **1987**, *26*, 138.

(12) Pei, Y.; Kahn, O.; Sletten, J.; Renard, J. P.; Georges, R.; Gianduzzo, J. C.; Curely, J.; Xu, Q. *Inorg. Chem.* **1988**, *27*, 47.

(13) Georges, R.; Curely, J.; Gianduzzo, J. C.; Xu, Q.; Kahn, O.; Pei, Y. *Physica B+C* **1988**, *153*, 77.

(14) Gleizes, A.; Verdaguer, M. *J. Am. Chem. Soc.* **1984**, *106*, 3727.

(15) Verdaguer, M.; Gleizes, A.; Renard, J. P.; Seiden, J. *Phys. Rev. B* **1984**, *29*, 5144.

(16) Journaux, Y.; Kahn, O.; Zarembowitch, J.; Galy, J.; Jaud, J. *J. Am. Chem. Soc.* **1983**, *105*, 7585.

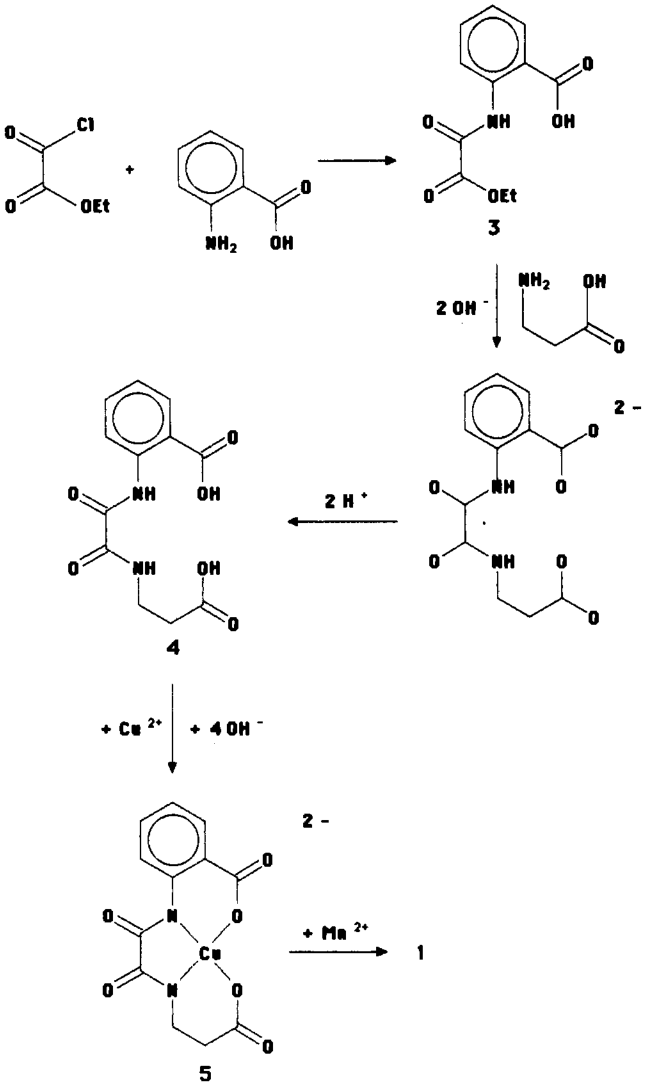

Figure 1. Synthesis scheme for $MnCu(obzp)(H_2O)_3{\cdot}H_2O$ (**1**).

chain compound with the characteristic minimum of $\chi_M T$ versus T plot, χ_M being the molar magnetic susceptibility per MnCu unit and T the temperature.[12] Due to weak interchain interactions, $MnCu(obp)(H_2O)_3{\cdot}H_2O$ exhibits a three-dimensional antiferromagnetic ordering at 2.3 K. The reaction of the latter copper(II) dianion with Mn(II) leads to two phases, $MnCu(obbz){\cdot}5H_2O$ and $MnCu(obbz){\cdot}H_2O$. The magnetic behavior of $MnCu(obbz){\cdot}5H_2O$ is very similar, qualitatively and quantitatively, to that of $MnCu(obp)(H_2O)_3{\cdot}H_2O$. As for $MnCu(obbz){\cdot}H_2O$, it exhibits a spontaneous magnetization below 14 K.[8,10]

To explore further this area of the alternating bimetallic chains, it seemed interesting to us to utilize dissymmetrical copper(II) precursors, i.e. compounds without a mirror plane perpendicular to the molecular plane. Along this line, we have synthesized the species $[Cu(obzp)]^{2-}$ with obzp = oxamido-*N*-benzoato-*N'*-propionato. The three precursors $[Cu(obp)]^{2-}$, $[Cu(obbz)]^{2-}$, and $[Cu(obzp)]^{2-}$ are represented as

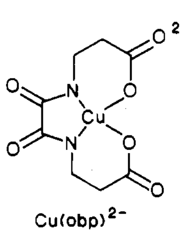

$Cu(obp)^{2-}$

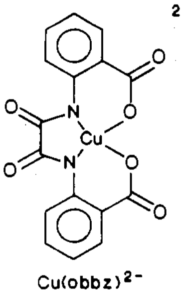

$Cu(obbz)^{2-}$

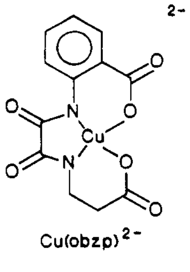

$Cu(obzp)^{2-}$

Table I. Crystallographic Data for $MnCu(obzp)(H_2O)_3{\cdot}H_2O$ (**1**)[a]

chem formula: $CuMnC_{12}H_{16}N_2O_{10}$	$Z = 4$
fw: 464.73	$T = 21$ °C
space group: $P2_1/n$ (No. 14)	$\lambda = 0.71073$ Å
$a = 7.814$ (1) Å	ρ(calc) = 1.933 g cm^{-3}
$b = 10.3375$ (7) Å	$\mu = 21.52$ cm^{-1}
$c = 19.981$ (1) Å	transm coeff: 0.39–0.63
$\beta = 98.43$ (1)°	$R(F_0) = 0.026$
$V = 1596.5$ (4) Å^3	$R_w(F_o) = 0.033$

[a] Atomic scattering factors and programs used are those of ref 22 and 23.

From $[Cu(obzp)]^{2-}$, we have obtained the bimetallic chain compound $MnCu(obzp)(H_2O)_3{\cdot}H_2O$ (**1**), of which the crystal structure has been solved. The magnetic susceptibility of this compound has been investigated and compared to the magnetic data obtained with $MnCu(obp)(H_2O)_3{\cdot}H_2O$.[12,13] In this paper, we also report on the synthesis and the magnetic properties of $MnCu(ophp){\cdot}4H_2O$ (**2**) obtained from the precursor $[Cu(ophp)]^{2-}$:

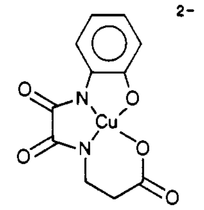

with ophp = oxamido-*N*-phenolato-*N'*-propionato.

Experimental Section

Syntheses. The synthesis of $MnCu(obzp)(H_2O)_3{\cdot}H_2O$ (**1**) was carried out in five steps according to the scheme shown in Figure 1. The first step consisted of preparing the ethyl oxamate benzoic acid compound **3**. For that, 10×10^{-3} mol of anthranilic acid was dissolved in 40 mL of THF. A 10×10^{-3} mol portion of ethyl oxalyl chloride in 10 mL of THF was then added dropwise. The mixture was refluxed for a while. The limpid solution was concentrated under vacuum, and **3** precipitated as a white powder. **3** was washed with water and dried under vacuum. The second step consisted of synthesizing the sodium salt of the organic ligand oxamido-*N*-benzoic acid-*N'*-propanoic acid (**4**). A 5×10^{-3} mol amount of **3** and 5×10^{-3} mol of NaOH were dissolved in 40 mL of methanol and added to 50 mL of a methanolic solution containing 5×10^{-3} mol of β-alanine and 5×10^{-3} mol of NaOH. The mixture was stirred overnight and then concentrated under vacuum. The sodium salt precipitated as a white powder. The third step consisted of obtaining **4**. For that, the sodium salt was redissolved in 40 mL of water. **4** precipitated when adding 12 N HCl. **4** was washed with water and dried under vacuum. The copper(II) species $Na_2[Cu(obzp)]{\cdot}3.5H_2O$ (**5**) was prepared in the fourth step as follows: 4×10^{-3} mol of **4** and 16×10^{-3} mol of NaOH were dissolved in 60 mL of water. A 10-mL amount of an aqueous solution containing 4×10^{-3} mol of copper(II) nitrate was then added. The resulting blue solution was filtered and reduced to 10 mL. Ethanol was then poured slowly into the filtrate, and **5** precipitated as a red polycrystalline powder. **5** was washed with ethanol and dried under vacuum. Anal. Calcd for $C_{12}H_{15}N_2O_{9.5}CuNa_2$: C, 32.11; H, 3.37; N, 6.24. Found: C, 32.09; H, 3.43; N, 6.02. Finally, well-shaped single crystals of $MnCu(obzp)(H_2O)_3{\cdot}H_2O$ (**1**) were obtained by slow diffusion in a H-shaped tube of two aqueous solutions, one containing 5×10^{-4} mol of **5** and the other one 5×10^{-4} mol of manganese(II) perchlorate. Anal. Calcd for $C_{12}H_{16}N_2O_{10}CuMn$: C, 30.88; H, 3.45; N, 6.00; O, 34.28; Cu, 13.62; Mn, 11.77. Found: C, 30.63; H, 3.19; N, 5.88; O, 34.11; Cu, 13.33; Mn, 11.67.

The synthesis of $MnCu(ophp){\cdot}5H_2O$ (**2**) was carried out in a way essentially similar to that for $MnCu(obzp)(H_2O)_3{\cdot}H_2O$ (**1**) by using 2-aminophenol instead of anthranilic acid in the first step. Anal. Calcd for $C_{11}H_{18}N_2O_{10}CuMn$: C, 28.93; H, 3.97; N, 6.13; Cu, 13.91; Mn, 12.03. Found: C, 29.19; H, 3.80; N, 6.43; Cu, 13.99; Mn, 11.72. Slow diffusion did not give single crystals suitable for X-ray work. Replacing manganese(II) perchlorate with nickel(II) perchlorate affords $NiCu(ophp){\cdot}4H_2O$. Anal. Calcd for $C_{11}H_{16}N_2O_9CuNi$: C, 29.85; H, 3.67; N, 6.39; Cu, 14.36; Ni, 13.26. Found: C, 29.87; H, 3.42; N, 6.72; Cu, 14.10; Ni, 13.19.

Data Collection and Structure Determination. Information concerning conditions for crystallographic data collection and structure refinement

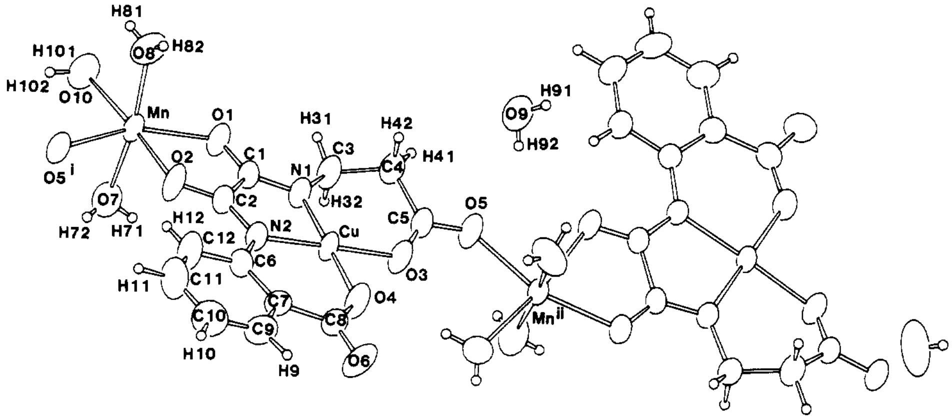

Figure 2. Section of chain in compound **1**. Thermal ellipsoids of non-hydrogen atoms are plotted at the 70% probability level. Hydrogen atoms are given an arbitrary radius.

Table II. Atomic Parameters for Non-Hydrogen Atoms of $MnCu(obzp)(H_2O)_3 \cdot H_2O$ (**1**)[a]

atom	*x*	*y*	*z*	B_{eq}, Å^2
Cu	0.35493 (3)	0.59829 (2)	0.55867 (1)	2.059 (5)
Mn	0.16542 (4)	0.82672 (3)	0.31372 (1)	2.028 (6)
O1	0.2747 (2)	0.8650 (1)	0.41639 (7)	2.53 (3)
O2	0.1377 (2)	0.6430 (2)	0.36741 (7)	3.00 (3)
O3	0.4872 (2)	0.6559 (1)	0.64560 (7)	2.88 (3)
O4	0.3538 (2)	0.4328 (1)	0.59848 (7)	3.03 (3)
O5	0.5761 (2)	0.7956 (2)	0.72688 (7)	2.87 (3)
O6	0.3139 (2)	0.2260 (2)	0.60777 (8)	3.20 (3)
O7	0.4243 (2)	0.7841 (2)	0.29131 (8)	3.73 (4)
O8	−0.0895 (2)	0.8936 (2)	0.32154 (9)	3.70 (4)
O9	0.2513 (3)	0.9331 (2)	0.76767 (9)	5.17 (5)
O10	0.1710 (2)	0.9999 (2)	0.24879 (8)	3.07 (3)
N1	0.3609 (2)	0.7640 (2)	0.51850 (8)	2.15 (3)
N2	0.2297 (2)	0.5426 (2)	0.47112 (8)	1.97 (3)
C1	0.2889 (3)	0.7693 (2)	0.45566 (9)	1.95 (4)
C2	0.2099 (3)	0.6404 (2)	0.42766 (9)	1.97 (4)
C3	0.4409 (3)	0.8800 (2)	0.5518 (1)	2.61 (4)
C4	0.4274 (3)	0.8836 (2)	0.6260 (1)	2.72 (4)
C5	0.5042 (3)	0.7706 (2)	0.6679 (1)	2.11 (4)
C6	0.1631 (3)	0.4171 (2)	0.4556 (1)	1.96 (4)
C7	0.1935 (3)	0.3166 (2)	0.5036 (1)	2.05 (4)
C8	0.2926 (3)	0.3264 (2)	0.5735 (1)	2.13 (4)
C9	0.1288 (3)	0.1926 (2)	0.4859 (1)	2.79 (4)
C10	0.0385 (3)	0.1652 (2)	0.4237 (1)	3.35 (5)
C11	0.0050 (3)	0.2633 (2)	0.3773 (1)	3.43 (5)
C12	0.0658 (3)	0.3870 (2)	0.3928 (1)	3.01 (5)

[a] The isotropic equivalent thermal parameter is given as $B_{eq} = {}^4/{}_3\sum_i\sum_j\beta_{ij}a_i \cdot a_j$.

Table III. Bond Distances Involving Non-Hydrogen Atoms in $MnCu(obzp)(H_2O)_3 \cdot H_2O$ (**1**)[a]

Cu–O3	1.977 (1)	O1–C1	1.257 (2)	C1–C2	1.538 (2)
Cu–O4	1.887 (1)	O2–C2	1.252 (2)	C3–C4	1.501 (2)
Cu–Ni	1.895 (1)	O3–C5	1.266 (2)	C4–C5	1.509 (2)
Cu–N2	1.961 (1)	O4–C8	1.271 (2)	C6–C7	1.409 (2)
Mn–O1	2.139 (1)	O5–C5	1.255 (2)	C6–C12	1.403 (2)
Mn–O2	2.206 (1)	O6–C8	1.240 (2)	C7–C8	1.498 (2)
Mn–O5^{i}	2.177 (1)	N1–C1	1.299 (2)	C7–C9	1.403 (2)
Mn–O7	2.179 (1)	N1–C3	1.465 (2)	C9–C10	1.365 (2)
Mn–O8	2.134 (1)	N2–C2	1.326 (2)	C10–C11	1.373 (3)
Mn–O10	2.214 (1)	N2–C6	1.415 (2)	C11–C12	1.383 (2)

[a] Symmetry operation: (i) $-^1/_2 + x, ^3/_2 - y, -^1/_2 + z$.

is summarized in Table I. The crystals of $MnCu(obzp)(H_2O)_3 \cdot H_2O$ are elongated reddish brown prisms, limited by the faces (100), (−100), (001), (0,0,−1), (011), (0,−1,−1), (0,1,−1), and (0,−1,1). Cell dimensions were determined from 25 reflections with 2θ angles between 17 and 25°. Three reference reflections were monitored throughout the data collection and showed no sign of deterioration. The data were corrected for absorption by a Gaussian integration method. The structure was solved by direct methods; the metal atoms and the coordinated atoms were revealed in the *E* maps, and the remaining non-hydrogen atoms were located in subsequent Fourier maps. After anisotropic refinement, hydrogen atoms were located in a difference map and were refined with isotropic thermal parameters. An extinction factor was included and ajusted. The refinement converged at $R = 0.026$, $R_w = 0.033$, $s = 2.24$. Atomic parameters for non-hydrogen atoms are listed in Table II. Anisotropic thermal parameters of non-hydrogen atoms are listed in Table SV and parameters of hydrogen atoms in Table SVI (supplementary material).

Magnetic Measurements. These were carried out with a Faraday-type magnetometer equipped with a helium continuous-flow cryostat in the 4–300 K temperature range, and with a laboratory-made low-field SQUID magnetometer in the 2–20 K temperature range. $HgCo(NCS)_4$ was used as a susceptibility standard. Diamagnetic corrections were taken as -250×10^{-6} cm^3 mol^{-1} for **1** and -230×10^{-6} cm^3 mol^{-1} for **2**.

EPR Spectra. The X-band powder EPR spectra of **1** and **2** were recorded at various temperatures between 4.2 and 300 K with a ER 200D Bruker spectrometer equipped with a helium continuous-flow cryostat, a Hall probe, and a frequency meter.

Description of the Structure of $MnCu(obzp)(H_2O)_3 \cdot H_2O$

The compound forms bimetallic chains running in the [101] direction. A section of a chain is shown in Figure 2. Bond lengths and angles involving non-hydrogen atoms are listed in Tables III and IV and those involving hydrogen atoms in Table SVII (supplementary material). Cu has approximately square-planar coordination, the equatorial positions being screened by the proximity of neighboring centrosymmetrically related molecules with Cu···N2($1 - x$, $1 - y$, $1 - z$) = 3.683 (1) Å and Cu···C11($-x$, $1 - y$, $1 - z$) = 3.555 (1) Å. Atomic deviations from the best plane through O3, O4, N1, and N2 are within ±0.003 Å with Cu located 0.022 Å from the plane. The two Cu–N bond distances are significantly different (1.895 and 1.961 Å) as are the Cu–O bond distances (1.887 and 1.977 Å). Mn has somewhat distorted octahedral surroundings, the two longest bond distances being to an oxamido oxygen atom and a water molecule in trans positions. A best least-squares plane through atoms O1, O2, O10, and O5^{i} (superscript i signifies the symmetry operation $-^1/_2 + x$, $^3/_2 - y$, $-^1/_2 + z$) reveals significant deviation from planarity, 0.083, −0.103, −0.069, and 0.089 Å, respectively, with Mn located −0.049 Å from this plane. Within the bimetallic chain, the Mn and Cu atoms are bridged by alternatively an oxamido group (O1, O2, N1, N2, C1, C2) with a Mn···Cu separation of 5.4376 (4) Å and a carboxylato group (O3, C5, O5) with a Mn···Cu separation of 5.3670 (4) Å. The Cu and Mn atoms deviate from the plane of the oxamido bridge by 0.012 and 0.203 Å, respectively, and by 0.209 and 0.163 Å from the plane of the carboxylato bridge. The equatorial planes of Cu (O3, O4, N1, N2) and Mn (O1, O2, O10, O5^{i}) make angles of 1.4 and 9.0° with the plane of the oxamido bridge and of 10.3° with each other. The carboxylato bridge makes angles of 17.0 and 14.5° with the equatorial planes of Cu and Mn^{ii} (O1^{ii}, O$_2$^{ii}, O5^{ii}, O10^{ii}), the dihedral angle between the last two planes being 29.1° (superscript ii signifies the symmetry operation $^1/_2 + x$, $^3/_2 - y$, $^1/_2 + z$).

The shortest metal···metal interchain separations occur (i) between copper atoms related by centers of symmetry, Cu···Cu($1 - x$, $1 - y$, $1 - z$) = 4.0375 (4) Å and Cu···Cu($-x$, $1 - y$, $1 - z$)

Table IV. Bond Angles Involving Non-Hydrogen Atoms in MnCu(obzp)$(H_2O)_3 \cdot H_2O$ (**1**)[a]

O3–Cu–O4	86.41 (4)	Mn–O1–C1	116.02 (9)	Ni–C3–C4	112.5 (1)
O3–Cu–N1	93.29 (4)	Mn–O2–C2	115.04 (9)	C3–C4–C5	116.6 (1)
O3–Cu–N2	178.28 (5)	Cu–O3–C5	127.25 (9)	O3–C5–O5	122.2 (1)
O4–Cu–Ni	178.82 (5)	Cu–O4–C8	130.05 (9)	O3–C5–C4	121.1 (1)
O4–Cu–N2	94.42 (5)	Mn^{ii}–O5–C5	132.5 (1)	O5–C5–C4	116.6 (1)
N1–Cu–N2	85.85 (5)	Cu–N1–C1	114.36 (9)	N2–C6–C7	120.5 (1)
O1–Mn–O2	75.35 (4)	Cu–N1–C3	125.59 (9)	N2–C6–C12	122.2 (1)
O1–Mn–O5^{i}	155.14 (4)	C1–Ni–C3	120.0 (1)	C7–C6–C12	117.4 (1)
O1–Mn–O7	88.97 (5)	Cu–N2–C2	110.81 (9)	C6–C7–C8	126.6 (1)
O1–Mn–O8	96.64 (5)	Cu–N2–C6	125.71 (9)	C6–C7–C9	118.9 (1)
O1–Mn–O10	111.87 (4)	C2–N2–C6	123.5 (1)	C8–C7–C9	114.4 (1)
O2–Mn–O5^{i}	81.06 (4)	O1–C1–N1	128.4 (1)	O4–C8–O6	119.6 (1)
O2–Mn–O7	94.91 (5)	O1–C1–C2	117.4 (1)	O4–C8–C7	122.5 (1)
O2–Mn–O8	94.84 (5)	N1–C1–C2	114.2 (1)	O6–C8–C7	117.9 (1)
O2–Mn–O10	172.64 (5)	O2–C2–N2	129.7 (1)	C7–C9–C10	122.4 (1)
O5^{i}–Mn–O7	85.29 (5)	O2–C2–C1	115.5 (1)	C9–C10–C11	118.9 (2)
O5^{i}–Mn–O8	93.01 (5)	N2–C2–C1	114.8 (1)	C10–C11–C12	120.4 (2)
O5^{i}–Mn–O10	91.98 (4)			C6–C12–C1	121.9 (2)
O7–Mn–O8	169.73 (6)				
O7–Mn–O10	86.84 (5)				
O8–Mn–O10	83.09 (5)				

[a] Symmetry operations: (i) $-^1/_2 + x, ^3/_2 - y, -^1/_2 + z$; (ii) $^1/_2 + x, ^3/_2 - y, ^1/_2 + z$.

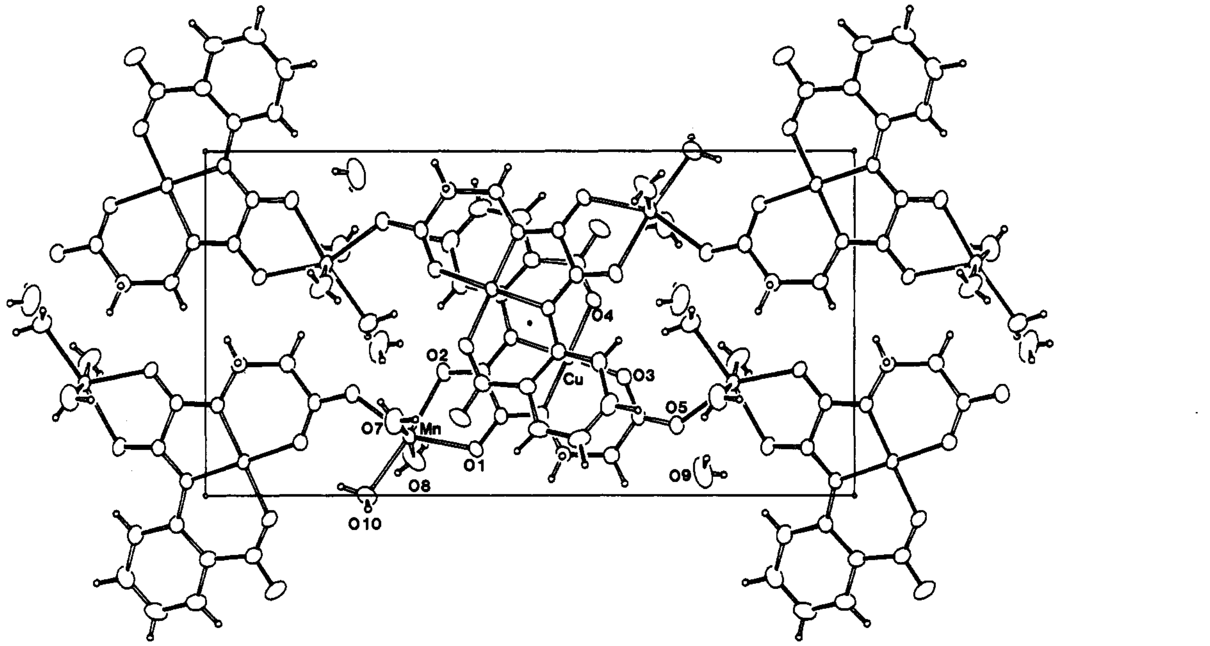

Figure 3. Crystal packing in compound **1**, projected down the *a* axis. The origin of the unit cell is in the upper left-hand corner.

= 6.0460 (4) Å, (ii) between copper and manganese in centrosymmetrically related chains, Cu···Mn$(1 - x, 1 - y, 1 - z)$ = 6.0844 (4) Å, and (iii) between manganese atoms related by a screw axis translation, Mn···Mn$(^1/_2 - x, ^1/_2 + y, ^1/_2 - z)$ = 5.9912 (4) Å. The crystal-packing pattern is illustrated in Figure 3. The chains are connected through hydrogen bonds, all potential donor sites being involved in such bonding. A list of hydrogen bonds is given in Table SVIII (supplementary material).

Let us compare now the structure of **1** to that of the previously described alternating bimetallic chain MnCu(obp)$(H_2O)_3 \cdot H_2O$.[12] In both compounds, the metal atoms are alternatively bridged by oxamido and carboxylato groups. The Cu···Mn distances across the carboxylato groups are, however, appreciably longer in the obp compound than in the compound **1** studied in this paper. This is due to different configurations at the carboxylato bridge; the configuration may be described as anti–anti in the obp compound and as anti–syn in compound **1**. We will see later on that this structure difference has dramatic consequences as far as the magnetic properties are concerned. Also the bond angle at the carboxylato oxygen atom bridging to Mn is 154.9° in the obp compound and 132.5° in **1**. In the obp compound, double chains are formed through a long axial Cu–O(carboxylato) bond, while compound **1** consists of single chains.

It is also interesting to compare the structure of **1** to that of NiCu(obbz)$(H_2O)_4 \cdot 2H_2O$, which has been previously reported.[10] The two compounds crystallize in the same space group with surprisingly similar cell dimensions, the main difference being the shorter *b* axis in **1**. The cell plots (see Figure 3 and Figure 2 of ref 10) reveal the similarity in the crystal packings. If the molecules in compound **1** are rotated a few degrees and slightly displaced, the carboxylato oxygen atom O5 in one molecule will come close to the coordinated water molecule O9 in a neighboring unit related by an *n* glide and, by comparison, in the chains of compound **1**, O5 in one asymmetric unit connects to Mn in the *n*-glide neighbor.

Magnetic Properties

The magnetic behaviors of **1** and **2** are qualitatively similar. The $\chi_M T$ versus T plot for **1** is shown in Figure 4. At room temperature, $\chi_M T$ is equal to 4.49 cm^3 mol^{-1} K, which is slightly below what is expected for isolated Mn(II) and Cu(II) ions. When the temperature is lowered, $\chi_M T$ continuously decreases and reaches a plateau around 10 K with $\chi_M T$ = 2.90 cm^3 mol^{-1} K. With a further decrease in temperature, $\chi_M T$ decreases again in a significant way and is equal to 2.53 cm^3 mol^{-1} K at 2 K. The key point of this magnetic behavior is that $\chi_M T$ versus T plot does

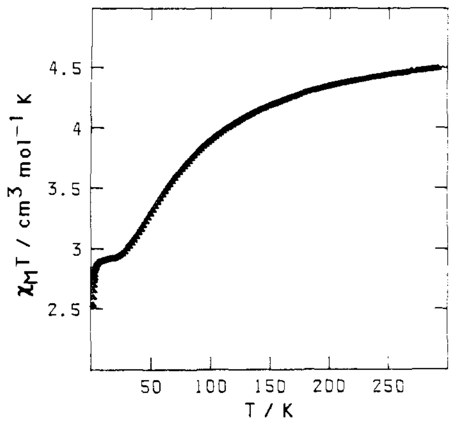

Figure 4. Experimental and calculated $\chi_M T$ versus T plots for compound **1**.

not exhibit the minimum expected for a ferrimagnetic chain.[3,17] In contrast, down to 6 K, it closely follows eq 1 valid for an isolated

$$\chi_M T = (2N\beta^2g^2/k)[5 + 14\exp(3J/kT)]/[5 + 7\exp(3J/kT)] \quad (1)$$

$Mn^{II}Cu^{II}$ pair with an antiferromagnetic intrapair interaction, where the symbols have their usual meaning. In such a pair, the interaction between the local $S_{Mn} = {}^5/_2$ and $S_{Cu} = {}^1/_2$ states gives rise to a ground $S = 2$ and an excited $S = 3$ pair states with a quintet-septet energy gap of $3J$ if the exchange Hamiltonian is written as $-JS_{Mn}\cdot S_{Cu}$. The plateau around 10 K corresponds to the temperature range where only the ground $S = 2$ state is thermally populated. $\chi_M T$ is then equal to $2N\beta^2 g_2^2/k$, g_2 being the average value of the Zeeman factor for this ground state. The least-squares fitting of the experimental data down to 6 K with eq 1 leads to $J = -27.4$ cm^{-1}, $g_2 = 1.97$, and $g_3 = 2.03$. The agreement factor defined as $\sum|(\chi_M T)^{obs} - (\chi_M T)^{calc}|^2/\sum|(\chi_M T)^{obs}|^2$ is then equal to 4×10^{-6}, which corresponds to an excellent agreement. g_2 and g_3 may be related to the local g factors g_{Mn} and g_{Cu}, assumed to be isotropic, through[3,18]

$$g_2 = (7g_{Mn} - g_{Cu})/6 \qquad g_3 = (5g_{Mn} + g_{Cu})/6 \quad (2)$$

g_{Mn} and g_{Cu} deduced from (2) are found equal to $g_{Mn} = 2.00$ and $g_{Cu} = 2.18$.

The decrease of $\chi_M T$ below the plateau could be due to either a zero-field splitting within the $S = 2$ ground state or antiferromagnetic interactions between $S = 2$ pair states. If the $Mn^{II}Cu^{II}$ pairs were magnetically isolated with a significant zero-field splitting, the compound would be EPR silent as the $Fe^{III}Cu^{II}$ pairs are.[3,16] It is actually not the case. The X-band powder EPR spectrum for **1** shows a single and symmetrical resonance centered at $g = 2.036$ (3). The line width is equal to 320 G at room temperature and does not vary significantly with the temperature.

The $\chi_M T$ versus T plot for **2** is shown in Figure S6 (supplementary material). The least-squares fitting of the experimental data with eq 1 for **2** leads to $J = -42$ cm^{-1}, $g_2 = 1.96$, and $g_3 = 2.06$. R is then equal to 3×10^{-5}.

Discussion and Conclusion

The compounds **1** and likely **2** have a structure of alternating bimetallic chains. However, they surprisingly behave as antiferromagnetically coupled $Mn^{II}Cu^{II}$ pairs. The magnitude of the interaction corresponds to what is expected for Mn^{II}–oxamido–Cu^{II} linkages. The ability of bisbidentate ligands like oxamido to transmit the electronic effects between metal centers far away from each other is now well documented.[19]

The most striking result of this study concerns the fact that the Mn^{II}–Cu^{II} interaction through the carboxylato bridge in **1** and **2** is negligible. This result contrasts with that observed in $MnCu(obp)(H_2O)_3\cdot H_2O$. In this latter compound, the J_2 interaction parameter through the carboxylato bridge was found equal to -6.8 (7) cm^{-1}. This difference is particularly spectacular as far as the low-temperature magnetic properties are concerned. Indeed, the $\chi_M T$ versus T plot for $MnCu(obp)(H_2O)_3\cdot H_2O$ exhibits at 40 K the minimum characteristic of ferrimagnetic chains whereas $\chi_M T$ for **1** and **2** tends to a plateau when T decreases, with a Curie constant corresponding to a $S = 2$ pair state. The structure of **2** is not known, but that of **1** has been determined, and it appears obvious that the difference of magnetic behaviors between $MnCu(obp)(H_2O)_3\cdot H_2O$ and **1** is related to the geometry changes of the Mn^{II}–carboxylato–Cu^{II} linkages. The configuration of the bridge is anti–anti in $MnCu(obp)(H_2O)_3\cdot H_2O$ and anti–syn in **1** as schematized in Figure 5.

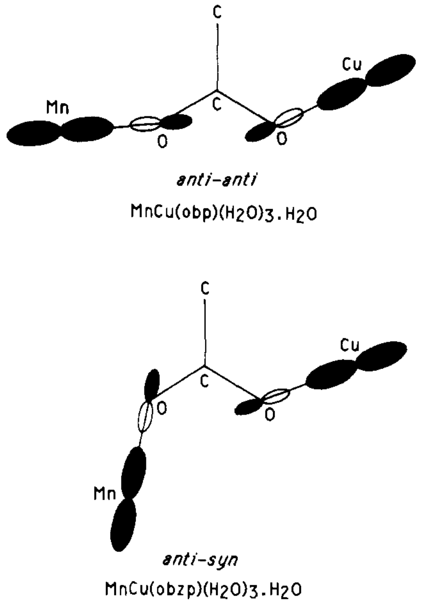

Figure 5. Orbital interactions between Mn(II) and Cu(II) ions through the carboxylato bridge with anti–anti and anti–syn configurations.

It is rather easy to justify qualitatively why the anti–anti configuration is more favorable than the anti–syn one to transmit the electronic effects. Indeed, the three magnetic orbitals involved in the Mn^{II}–Cu^{II} antiferromagnetic interaction are of the $d_{x^2-y^2}$ and d_{z^2} type around Mn(II) (the local z axis being taken along the apical direction, i.e. O7MnO8 in **1**) and of the $d_{x^2-y^2}$ type around Cu(II). The first two orbitals point along the the Mn–O directions in the equatorial plane (MnO1O2O10O5^i in **1**). The third one points along the Cu–N and Cu–O directions in the equatorial plane (CuN1N2O3O4 in **1**). These orbitals are delocalized toward the 2p oxygen orbitals of the carboxylato bridge (see Figure 5). The two 2p oxygen orbitals are much more favorably oriented to overlap in the anti–anti configuration than in the anti–syn configuration. It can also be noticed that these two 2p oxygen orbitals overlap with the same 2p carbon orbital in the anti–anti case and with different 2p carbon orbitals in the anti–syn case, which results in a better overlap of the magnetic orbitals in the former case than in the latter. Of course, such an approach is oversimplified and does not consider the highest occupied molecular orbitals of the carboxylato group as a whole; it is based on a model in which the magnitude of the antiferromagnetic interaction is governed by the overlaps between magnetic orbitals.[3] To our knowledge, there is no other qualitative model valid for such an interaction involving different metal ions and a bridging network of low symmetry. There is at least another magnetic system with acetato groups bridging in an anti–syn fashion;[20,21] this system is $[Cu(NH_3)_2(CH_3COO)Br]$, and the

---

(17) Verdaguer, M.; Julve, M.; Michalowicz, A.; Kahn, O. *Inorg. Chem.* **1983**, *22*, 2624.

(18) Scaringe, R. P.; Hodgson, D.; Hatfield, W. E. *Mol. Phys.* **1978**, *35*, 701.

(19) Kahn, O. *Angew. Chem., Int. Ed. Engl.* **1985**, *24*, 834.

(20) Ferrari, M. B.; Capacchi, L. C.; Fava, G. G.; Nardelli, M. *J. Cryst. Mol. Struct.* **1972**, *2*, 291.

(21) Carlin, R. L.; Kopinga, K.; Kahn, O.; Verdaguer, M. *Inorg. Chem.* **1986**, *25*, 1786.

interaction between Cu(II) ions is characterized by $J = -6$ cm^{-1}, which is quite a small value, in particular when compared to the interaction in copper(II) acetate, where four acetato groups bridge in a syn–syn fashion. It is also worth noting that the comparison between MnCu(obp)$(H_2O)_3 \cdot H_2O$ and **1** confirms, if it was still necessary, that the magnitude of the interaction is not directly related to the separation between the magnetic centers. As a matter of fact, due to the anti–syn configuration, the Mn···Cu distance across the carboxylato bridge is much shorter in **1** than in MnCu(obp)$(H_2O)_3 \cdot H_2O$ (5.3670 (4) Å and 6.066 (2) Å, respectively).

In the discussion, we have implicitly assumed, so far, that the Mn^{II}–Mn^{II} and Cu^{II}–Cu^{II} intrachain interactions between next nearest neighbor metal ions were negligible. This assumption could not be rigorously valid. Perhaps the observed magnetic behavior results from a subtle balance between a weak Mn(II)–Cu(II) antiferromagnetic interaction through the carboxylato bridge favoring the one-dimensional ferrimagnetism and weak Mn(II)–Mn(II) and/or Cu(II)–Cu(II) antiferromagnetic interactions involving next nearest neighbors and favoring one-dimensional antiferromagnetism. The Mn(II)–Mn(II) dipolar interactions between high local spins could also play a role.

As already mentioned, our goal in this field of the bimetallic chains is both to obtain the one-dimensional ferrimagnetic behavior and to design molecular compounds exhibiting a spontaneous magnetization. To date, three compounds have already been investigated. One behaves as a one-dimensional ferrimagnet, with a three-dimensional ordering at very low temperature, another one exhibits a spontaneous magnetization below 14 K, and the third one behaves magnetically as isolated Mn^{II}Cu^{II} pairs with oxamido bridges. The EPR spectra, however, show that the pairs are not perfectly isolated but weakly interact through the carboxylato bridges, in agreement with the crystal structure.

Acknowledgment. We express our deepest gratitude to the Sociêté Nationale Elf Aquitaine, which has financially supported this work and offered a research grant to K.N.

Supplementary Material Available: Tables SV–SVIII, listing anisotropic thermal parameters for non-hydrogen atoms, hydrogen atomic parameters, bond distances and angles involving hydrogen atoms, and hydrogen bonds for MnCu(obzp)$(H_2O)_3 \cdot H_2O$ (**1**), and Figure S6, giving the $\chi_M T$ versus T plot for MnCu(ophp)$\cdot 5H_2O$ (**2**) (5 pages); a table of structure factors for MnCu(obzp)$(H_2O)_3 \cdot H_2O$ (**1**) (17 pages). Ordering information is given on any current masthead page.

---

(22) Cromer, D. T.; Waber, J. T. *International Tables for X-Ray Crystallography*; Kynoch Press: Birmingham, England, 1974; Vol. IV, p 99, Table 2.2B.

(23) Frenz, B. a. *The SDP-User's Guide*; Enraf-Nonius: Delft, The Netherlands, 1983.

Contribution from the Department of Chemistry, University of Florence, via Maragliano 75/77,
50144 Florence, Italy, Department of Energetics, University of Florence, Santa Marta, Florence, Italy,
and Department of Inorganic Chemistry, University of Valencia, Valencia, Spain

Nickel(II) Complexes of [3*k*]aneN$_k$ Polyazacycloalkanes (k = 7–12). Solution and Solid-State Studies

Andrea Bencini,[1a] Antonio Bianchi,*[1a] Manuel Castelló,[1b] Paolo Dapporto,[1c] Juan Faus,*[1b]
Enrique Garcia-España,*[1b] Mauro Micheloni,*[1a] Piero Paoletti,*[1a] and Paola Paoli[1a]

Received November 28, 1988

A potentiometric study of the equilibria between nickel(II) and the large polyazacycloalkanes of the series [3*k*]aneN$_k$ (k = 7–12) has been carried out at 25 °C in 0.15 mol dm^{-3} NaClO$_4$–water solution as ionic medium. The ligand [21]aneN$_7$ forms only mononuclear complexes, while [24]aneN$_8$ forms both mononuclear and binuclear complexes. Only binuclear complexes are formed when k = 9–12. The stability of the mononuclear complexes is compared with that previously reported for complexes formed by smaller macrocycles (k = 3–6). The equilibrium constants of mononuclear complexes increase on going from [9]aneN$_3$ to the hexadentate [18]aneN$_6$ and then decrease for [21]aneN$_7$ (log K = 16.563 (5)) and [24]aneN$_8$ (log K = 13.94 (5)). The stability of binuclear complexes increases with the dimension of the ligands and the number of donor atoms: [24]aneN$_8$ (log K = 23.30 (1)); [27]aneN$_9$ (log K = 26.24 (1)); [30]aneN$_{10}$ (log K = 30.02 (3)); [33]aneN$_{11}$ (log K = 31.07 (1)); [36]aneN$_{12}$ (log K = 32.09 (3)). Many protonated species are formed, and their equilibrium constants have been measured. Also hydroxodinickel(II) complexes have been detected. Magnetic properties of solid complexes and electronic spectra of these compounds, both in the solid state and in solution, are indicative of high-spin octahedral nickel(II) complexes. Only in the case of [24]aneN$_8$ has a dinickel(II) diamagnetic square complex ([Ni$_2$([24]aneN$_8$)](ClO$_4$)$_4$) been isolated. This compound dissolves in water to produce, over a period of some hours, octahedral species. The molecular structure of the dinickel(II) complex [Ni$_2$([30]aneN$_{10}$)(H$_2$O)$_2$](NO$_3$)$_4$ ([30]aneN$_{10}$ = 1,4,7,10,13,16,19,22,25,28-decaazacyclotriacontane) has been determined by single-crystal X-ray analysis. This compound crystallizes in the $P2_1/a$ space group with a = 13.894 (2) Å, b = 9.386 (6) Å, c = 14.100 (2) Å, β = 113.13 (2)°, and Z = 2. Refinement of the atomic parameters by least squares gave a final R factor of 0.065 (R_w = 0.056) for 2140 unique reflections having $I \geq 3\sigma(I)$. The structure consists of centrosymmetric [Ni$_2$([30]aneN$_{10}$)(H$_2$O)$_2$]$^{4+}$ cations and uncoordinated nitrate anions. The nickel(II) ion of the complex cation is coordinated by five nitrogen atoms of the macrocyclic ligand and one water molecule in a distorted octahedral environment. Also, the crystalline compound [Ni([21]aneN$_7$)](ClO$_4$)$_2$ has been analyzed by X-ray diffractometry. Crystals of this compound are orthorhombic, space group $P22_12_1$, with a = 9.692 (4) Å, b = 14.872 (1) Å, c = 32.366 (3) Å, and Z = 8. Only the two independent nickel(II) ions of two different molecules, the non-hydrogen atoms of a [Ni([21]aneN$_7$)]$^{2+}$ cation, and the four perchlorate anions were localized. Any attempt to localize the atoms of the macrocycle of the second complex cation was unsuccessful because of the disorder of this molecule; refinement of atomic parameters by least squares was interrupted (R factor about 20% for the 2395 reflections having $I \geq 3\sigma(I)$). The nickel(II) ion in the [Ni([21]aneN$_7$)]$^{2+}$ cation is coordinated by six nitrogen atoms of the ligand, one nitrogen remaining uncoordinated in an eight-membered chelate ring.

Introduction

It is a general idea in the synthesis of macrocyclic ligands to produce molecules in which one or more metal ions could be readily coordinated. Anyhow, in some cases, metal ions have to be forced to enter into the macrocyclic cavity. A classic example is offered by nickel(II) with some tetraazacycloalkanes, for which the reaction of complexation in water is fast only at high temperatures.[2–4] The resulting complexes are characterized by a surprising ther-

---

[1] (a) Department of Chemistry, University of Florence. (b) University of Valencia; c/o Dr. Moliner, 50, 46100 Burjassot, Valencia, Spain. (c) Department of Energetics, University of Florence.

[2] Kaden, T. A. *Helv. Chim. Acta* **1970**, *53*, 617. Steinmann, W.; Kaden, T. A. *Helv. Chim. Acta* **1975**, *58*, 1358 and references therein.

[3] Busch, D. H. *Acc. Chem. Res.* **1978**, *11*, 392.

[4] Hay, R. W.; Norman, P. R. *Inorg. Chim. Acta* **1980**, *45*, L139.